

Induced nanoscale deformations in polymers using atomic force microscopy

Sergei F. Lyuksyutov* and Pavel B. Paramonov

Departments of Physics and Polymer Engineering, The University of Akron, Akron, Ohio 44325, USA

Ruslan A. Sharipov

Department of Mathematics, Bashkir State University, 32 Frunze St, Ufa 450074, Russia

Grigori Sigalov

Department of Computer Science, Virginia Tech University, Blacksburg, Virginia 24061, USA

(Received 9 February 2004; revised manuscript received 1 June 2004; published 19 November 2004)

An exact analytical solution, based on the method of images, is obtained for the description of the electric field between an atomic force microscope (AFM) tip and a thin dielectric polymer film (30 nm thick) spin coated on a conductive substrate. Three different tip shapes are found to produce electrostatic pressure above the plasticity threshold in the polymers up to 50 MPa. It is shown experimentally that a strong nonuniform electric field ($5 \times 10^8 - 5 \times 10^9 \text{ V m}^{-1}$) between the AFM tip and polymer substrate produces nanodeformations of two different kinds in planar polymer films. Nanostructures (lines and dots) 10–100 nm wide and 0.1–5 nm high are patterned in the polymer films by using two different experimental techniques. The first technique relies on electric breakdown in the film leading to polymer heating above the glass transition point followed by mass transport of softened polymer material towards the AFM tip. The second technique is believed to be associated with plastic deformation of the polymer surface at the nanoscale. In this case the nanostructures are experimentally patterned in the films with no external biasing of the AFM tip, and using only the motion of the tip. This suggests an additional nanomechanical approach for nanolithography in polymer films of arbitrary thickness.

DOI: 10.1103/PhysRevB.70.174110

PACS number(s): 68.47.Mn, 68.37.Ps, 81.16.Rf

INTRODUCTION

The conceptual development of nanolithography techniques for surface modification of inorganic, organic, and polymeric materials is of great importance for progress in such areas as data storage, nanoscale electronics and optoelectronics, sensors, and spatially controlled chemical synthesis. A number of nanolithography approaches have been developed during the last decade,¹ which differ in resolution, speed, and complexity of the implementation in polymers.

Lithographically induced self-construction in polymer materials, pioneered by Chou *et al.*² is based on capillary instability of polymer surface above the glass transition point. A physical explanation of polymer dielectric liquid instability in strong electric field ($10^7 - 10^8 \text{ V m}^{-1}$) induced between capacitor plates was suggested by Herminghaus.³ The technique was implemented by Schaeffer *et al.*,⁴ and is based on competing forces at the polymer liquid-air interface. When the temperature of a polymer film is raised above the glass transition temperature using an external heating device, the film turns it into a liquid while a strong electric field polarizes a dielectric polymer liquid. This results in instability of the film due to the displacement of space charge competing against surface tension force that minimizes the area of the interface. When electrostatic and van der Waals' pressure overcomes Laplace pressure, associated with surface tension, the film becomes highly unstable in responding to small perturbations, and moves along the electric field lines

to one of the plates. Since this effect is associated with the growth of instability in the liquid, it is a very slow process and requires hours to form nanostructures. This approach has been further developed by Russell and co-workers for nanostructure formation in bilayer polymer films at resolution around 100 nm.^{5,6}

Atomic force microscopy (AFM) has been proven to be an extremely useful tool for polymer surface modification. Data storage in polymers based on AFM thermomechanical writing was developed by Mamin and Rugar.⁷ This resulted in an industrial prototype called MILLIPEDE with storage capacity up to 620 bits/ μm^2 .⁸ Orientational ordering of a polymer surface by an unbiased AFM tip was reported by Leung and Goh,⁹ and also by Keneko,¹⁰ although no explanation was provided for the effect at that time.

Recently, an alternative approach for data storage on the nanoscale based on electronic breakdown through 10–40-nm-polymer films spin coated on conductive substrates has been suggested. Application of a bias voltage (5–50 V) between a conductive AFM tip (or the arrays of the tips) and the substrate resulting in charge transport (due to the breakdown) and also in localized Joule heating of (nano-) amounts of polymer. Electrostatic attraction of the softened polymer film toward the AFM tips produces nanostructures with dimensions (5–100 nm width and 0.1–100 nm height). This AFM-based electrostatic nanolithography (AFMEN) technique, developed by Lyuksyutov and Vaia with co-workers,^{11,12} offers several advantages with

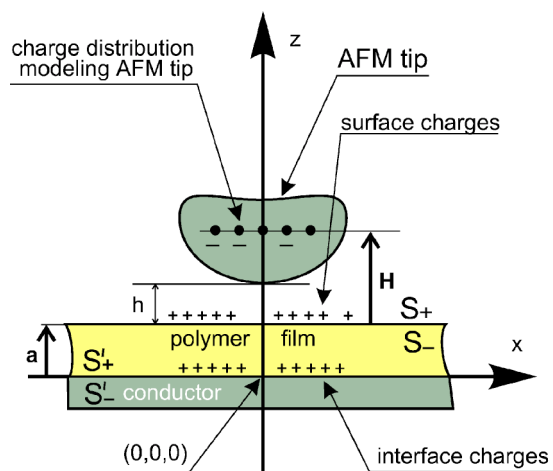


FIG. 1. (Color online) Schematic representation of the electrostatic field formation between an AFM tip and a conductive layer with a polymer film spin-coated onto the conductor. The thickness of the polymer film is 30 nm. The method of images was used to determine the field (in the range of 5×10^8 – 10^9 V m $^{-1}$), and an electrostatic pressure that deforms the polymer film. The electric charges are concentrated either on the interface S' resulting in electronic breakdown, or on the interface S resulting in plastic deformation.

respect to all the existing methods, such as fast time of nanostructures formation (less than 1 μ s), and applicability to a broad class of polymer materials that can be patterned using the AFMEN technique.

The motivation for writing the present paper was the development of an electrostatic model describing interactions in the system comprised of an AFM tip (electrically biased or not) of different various shapes and a slab of thin dielectric material spin-coated on a conductive surface. Prior to the present work there was no clear image describing electric charge exchange between a conducting AFM tip and a thin insulator film leading to the modification of the polymer surface either through the electric breakdown and heating (AFMEN), or the plastic–elastic deformation on nanoscale.

The prime goal of this paper is to use the method of images to derive the exact analytical solution for the electric field and the electrostatic pressure associated with this field which results in nanostructures formation due to the electrostatic pressure for a system consisting of a charged AFM tip, a dielectric polymer film, and a conductor. The solution will provide a major step towards a general phenomenological description of the fields, and the electrostatic pressure formation inside and outside the polymer film. A complementary goal is to provide experimental evidence to support the solution.

THEORETICAL

A conceptual presentation of the conductive AFM tip above the polymer film spin-coated on the conductive substrate is shown in Fig. 1. A conductive AFM tip is presented as an equipotential surface of the electrostatic field created through electric charge distributed above and/or on the poly-

mer film surface S . The charge distribution produces the electric field $\mathbf{E}_0(\mathbf{r})$ in free space. The method of images is applied to solve for the electric field configuration produced by this charge distribution in the presence of a thin polymer film coated on a conductive substrate.¹³ The method of images is a convenient instrument to analyze tip–surface interactions. It has been used for the analysis of polymer elastic properties by Dimitriadis *et al.*,¹⁴ although it has never been used to solve for the electric field distribution in this geometry. The actual electrostatic field inside [$\mathbf{E}_{in}(\mathbf{r})$], and outside [$\mathbf{E}_{out}(\mathbf{r})$] the film are solved separately¹³ results in the following formulas:

$$\mathbf{E}_{in}(\mathbf{r}) = (1 - \eta) \sum_{n=0}^{\infty} (-\eta)^n [\mathbf{E}_0(\mathbf{r} - 2n\mathbf{a}) - \mathbf{E}_0^*(\mathbf{r}^* - 2n\mathbf{a})], \quad (1)$$

$$\mathbf{E}_{out}(\mathbf{r}) = \mathbf{E}_0(\mathbf{r}) - \eta \mathbf{E}_0^*(\mathbf{r}^* + 2\mathbf{a}) - (1 - \eta^2) \sum_{n=0}^{\infty} (-\eta)^n \times \mathbf{E}_0^*(\mathbf{r}^* - 2n\mathbf{a}). \quad (2)$$

Here $\mathbf{r} = (x, y, z)$ and $\mathbf{r}^* = (x, y, -z)$ are the radii vectors of the coordinate system with origin at the polymer film and conductive substrate interface (see Fig. 1); $\mathbf{E}_0 = (E_{01}, E_{02}, E_{03})$ and $\mathbf{E}_0^* = (E_{01}, E_{02}, -E_{03})$ are the electrostatic field vectors in free space; $\eta = \epsilon - 1 / \epsilon + 1$ where ϵ is the dielectric permittivity of the polymer film.¹⁵ The vector \mathbf{a} is directed along the z axis, and $a = |\mathbf{a}|$ is the height of the polymer film. An asterisk above the vectors indicates that the mirror reflection operator is executed with respect to the plane S' acting as a mirror.

For further consideration two different cases must be distinguished: (1) When the AFM tip is positioned at a distance comparable ($h \leq a$) with the polymer film height, and (2) when it is at a separation smaller than the film height ($h \ll a$).

In the first case, the conductive AFM tip is presented as a point charge Q producing a Coulombic electric field $\mathbf{E}_0(\mathbf{r})$:

$$\mathbf{E}_0(\mathbf{r}) = \frac{1}{4\pi\epsilon_0} \cdot \frac{\mathbf{r} - (\mathbf{a} + \mathbf{H})}{|\mathbf{r} - (\mathbf{a} + \mathbf{H})|^3}. \quad (3)$$

The vector \mathbf{H} is along the z axis with magnitude equal to the polymer surface–electric charge(s) distance. Substituting Eq. (3) in (1) and (2) we arrive with the formulas for the electric field $\mathbf{E}(\mathbf{r})$ inside and outside of the polymer film:

$$\mathbf{E}_{in}(\mathbf{r}) = (1 - \eta) \frac{Q}{4\pi\epsilon_0} \sum_{n=0}^{\infty} (-\eta)^n \left(\frac{\mathbf{r} - [\mathbf{H} + (2n + 1)\mathbf{a}]}{|\mathbf{r} - [\mathbf{H} + (2n + 1)\mathbf{a}]|^3} - \frac{\mathbf{r} - [\mathbf{H} + (2n + 1)\mathbf{a}]}{|\mathbf{r} - [\mathbf{H} + (2n + 1)\mathbf{a}]|^3} \right), \quad (4)$$

$$\mathbf{E}_{\text{out}}(\mathbf{r}) = \frac{Q}{4\pi\epsilon_0} \left(\frac{\mathbf{r} - (\mathbf{H} + \mathbf{a})}{|\mathbf{r} - (\mathbf{H} + \mathbf{a})|^3} - \eta \frac{\mathbf{r} - (\mathbf{H} - \mathbf{a})}{|\mathbf{r} - (\mathbf{H} - \mathbf{a})|^3} \right) - (1 - \eta^2) \frac{Q}{4\pi\epsilon_0} \sum_{n=0}^{\infty} (-\eta)^n \frac{\mathbf{r} + (\mathbf{H} + \mathbf{a})}{|\mathbf{r} + (\mathbf{H} + \mathbf{a})|^3}. \quad (5)$$

The sum of the vectors $\mathbf{a} + \mathbf{H}$ is the radius vector of point charge Q . The mirror charges located at the points $\mathbf{H} + (2n + 1)\mathbf{a}$ and $-\mathbf{H} - (2n + 1)\mathbf{a}$ arise due to the set of mirror images in a recursive way. The scalar quantity $h = |\mathbf{h}|$ is the tip-polymer distance.

The electric field polarizes the polymer film so that its degree of polarization is described through the induced density of the dipole moment \mathbf{P} , where \mathbf{P} is given by: $\mathbf{E}_\sigma(\mathbf{r} \in S_+) - \mathbf{E}_\sigma(\mathbf{r} \in S_-) = \mathbf{n} \cdot \mathbf{P} / \epsilon_0 = \epsilon_0(\epsilon - 1)\mathbf{E}_{\text{in}}(\mathbf{r})$. The bulk and surface charge distributions appear as a result of polarization induced by the electric field: $\rho = -\nabla \cdot \mathbf{P}$, and $\sigma = \mathbf{P} \cdot \mathbf{n}$ for the volume and surface charge density, respectively, where \mathbf{n} is the unit vector normal to the surface S . The fact that the dielectric permittivity is constant yields $\nabla \cdot \mathbf{E} = 0$, and $\nabla \cdot \mathbf{P} = 0$, which implies no volume electric charge inside the polymer film. Using Gauss' theorem, the electric field $\mathbf{E}_\sigma(\mathbf{r})$ due to the surface charge on the plane S is presented as: $\mathbf{E}_\sigma(\mathbf{r} \in S_+) - \mathbf{E}_\sigma(\mathbf{r} \in S_-) = \sigma / \epsilon_0 \mathbf{n}$. This field must be subtracted from the expression for the net electrostatic field in Eqs. (4) and (5) to exclude self-action when calculating tension forces and pressure associated with the field. The pressure acting on the upper surface of the polymer film determines traction represented as: $\mathbf{T} = \sigma(\mathbf{E} - \mathbf{E}_\sigma)$. The surface charge density $\sigma = \sigma_{\text{pol}} = \epsilon_0(\epsilon - 1)\mathbf{E}_{\text{in}}^\perp(r)$ is determined by polarization charges solely (σ_{pol}), where $\mathbf{r} \in S$. The following two formulas present the tangential and normal components of stress (traction) occurring inside the polymer film. Although the formulas are invariant with respect to the sign of the electric charge, we further presume that the negative electric charge is concentrated on the AFM tip, and the positive charge is concentrated on the lower inner surface of the polymer film for $r \leq S_-$ (shown as interface charges in Fig. 1).

$$\mathbf{T}^\parallel = \epsilon_0(\epsilon - 1)\mathbf{E}_{\text{in}}^\perp \mathbf{E}_{\text{in}}^\parallel$$

$$\mathbf{T}^\perp = \epsilon_0 \left(\frac{\epsilon^2 - 1}{2} \right) \mathbf{E}_{\text{in}}^\perp \mathbf{E}_{\text{in}}^\perp. \quad (6)$$

Where, $\mathbf{E}_{\text{in}}^\perp$, and $\mathbf{E}_{\text{in}}^\parallel$ are the normal and tangential components of the electric field inside the polymer film. The second formula in Eq. (6) determines the traction created by the electrostatic field normal to the polymer surface. This expression is most important for further consideration.

In this case ($a \geq h$), a negative bias of several volts of the AFM tip produces conditions for the electric breakdown through the polymer film provided that the magnitude of the field exceeds the breakdown threshold. Based on experimental evidence of such a breakdown in thin polymer films of polymethylmethacrylate (PMMA) and polystyrene (PS), occurring for electric fields in the range between 5×10^8 and $5 \times 10^9 \text{ V m}^{-1}$ when the tip is based -10 – 20 V with respect to conductive Au–Pd substrate,^{11,12} we can calculate the electrostatic pressure acting on the softened polymer as a result

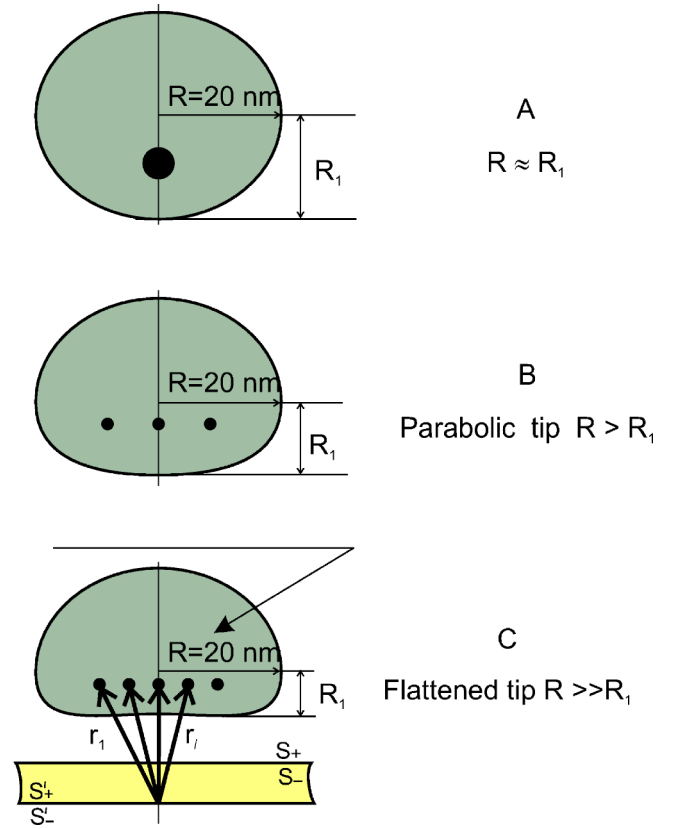


FIG. 2. (Color online) Three different tip configurations were used to solve for the electric field distribution: (a) almost spherical tip modeled by a point charge Q ; (b) parabolic tip modeled through a rare grid of the electric charges; (c) flattened tip modeled by a dense grid of the electric charges. The distance between the tip and a polymer surface was varied between 0.5 and 10 nm.

of this breakdown. The height of the film is assumed to be $a = 30 \text{ nm}$, and the tip-polymer distance $h = 5 \text{ nm}$, and 10 nm . With a tip voltage of -20 V electric fields of magnitude 4×10^9 and $2 \times 10^9 \text{ V m}^{-1}$, respectively, are created in the upper part of the film. We assume no substantial variation of the electric field inside the film because no field screening from the upper part of the polymer film occurs. Experimental results indicate that a softened polymer flow occurs forming raised nanostructures inside the cylinder of radius comparable or less the tip radius (20–40 nm radius).¹⁶ The results of the tensile stress (or electrostatic pressure) calculation (\mathbf{T}^\perp) as a function of distance x for three different tip shapes are seen in Figs. 3(a) and 3(b). It is shown that as the tip-polymer surface distance (h) increases, wider nanostructures are formed. Additionally, the tip shape does not strongly affect the pressure distribution.

In the second case the tip is positioned very close to the surface of the polymer ($h \ll a$) and its shape becomes important. Three different tip shapes, as presented in Fig. 2, have been studied. To model an almost spherical tip only a single charge positioned at the distance $\mathbf{R}_1 \approx \mathbf{R}$ inside the sphere of radius \mathbf{R} (tip radius) is required. A grid of point charges Q_1, \dots, Q_N positioned at the distance $\mathbf{R}_1 \ll \mathbf{R}$ was used to model parabolic [Fig. 2(b)], and flattened [Fig. 2(c)] tips respectively. These charges, together with the surface charges,

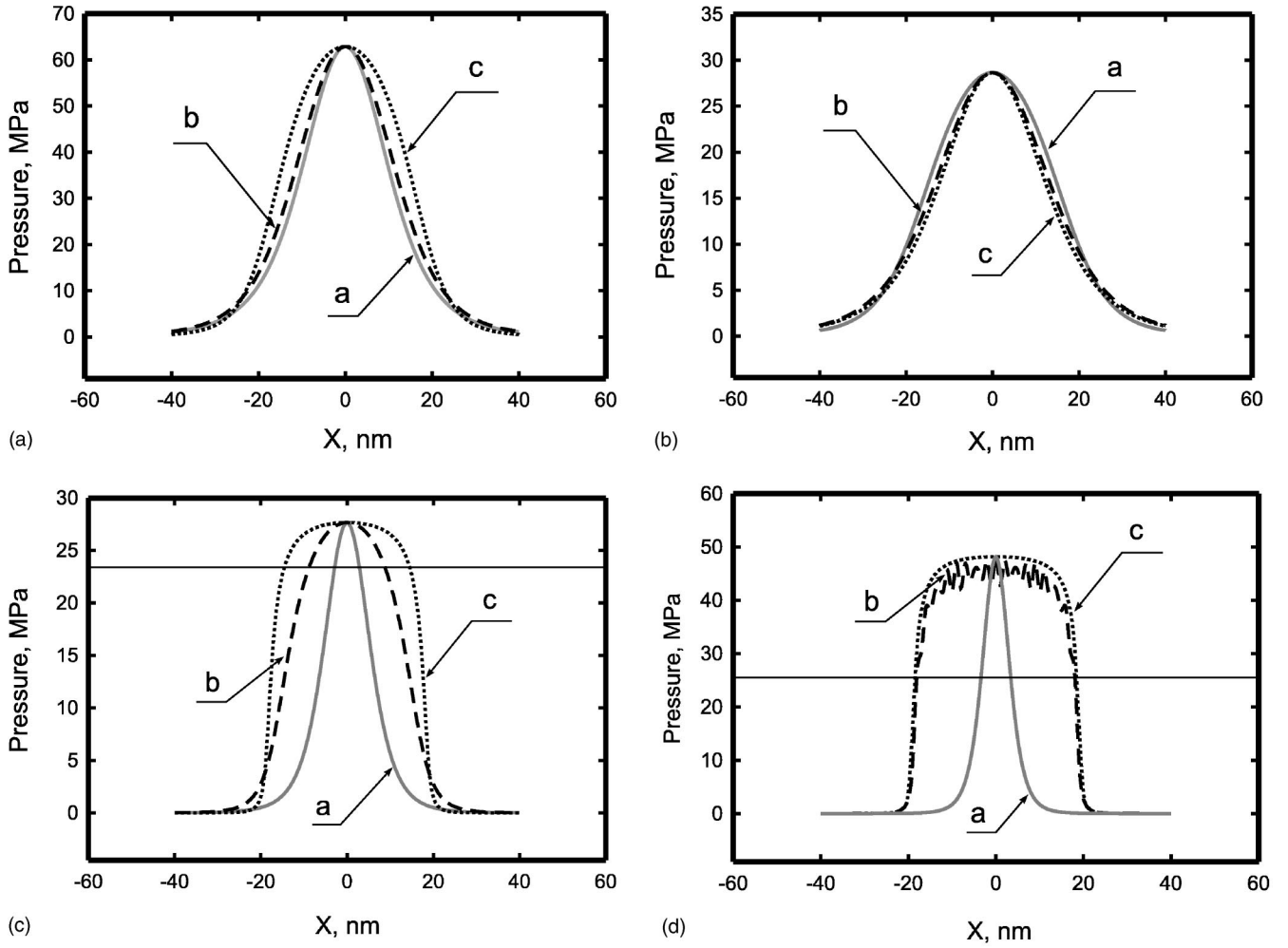


FIG. 3. Pressure creating deformation in a polymer film with respect to the distance in AFMEN case (charges concentrated on the interface S'): (a) The electric field magnitude $E=4 \times 10^9 \text{ V m}^{-1}$, for the tip-polymer surface separation $h=5 \text{ nm}$ (b) electric field magnitude $E=2.7 \times 10^9 \text{ V m}^{-1}$, for the tip-polymer surface separation $h=10 \text{ nm}$; pressure vs distance for surface charges concentrated on the interface S ; (c) the electric field magnitude $E=2.5 \times 10^9 \text{ V m}^{-1}$, for the tip-polymer surface separation $h=0.5 \text{ nm}$; (d) the electric field magnitude $E=3.3 \times 10^9 \text{ V m}^{-1}$, for the tip-polymer surface separation $h=0.3 \text{ nm}$; the horizontal line corresponds to the plastic deformation threshold $P=25 \text{ MPa}$. The curves (a), (b), and (c) correspond to the different AFM tip shapes presented in Fig. 2.

produce the basic electric field $\mathbf{E}_0(\mathbf{r}) = \sum_{i=1}^N \mathbf{E}_{i0}(\mathbf{r})$ where each summand is given by the following formula:

$$\mathbf{E}_{i0}(\mathbf{r}) = \begin{cases} \frac{(1-k)Q_i}{4\pi\epsilon_0} \frac{\mathbf{r} - \mathbf{r}_i}{|\mathbf{r} - \mathbf{r}_i|^3} & \text{for } z < a \\ \frac{Q_i}{4\pi\epsilon_0} \cdot \frac{\mathbf{r} - \mathbf{r}_i}{|\mathbf{r} - \mathbf{r}_i|^3} - \frac{kQ_i}{4\pi\epsilon_0} \cdot \frac{\mathbf{r} - \mathbf{r}'_i}{|\mathbf{r} - \mathbf{r}'_i|^3} & \text{for } z > a \end{cases}, \quad (7)$$

Where $\mathbf{r}_1, \dots, \mathbf{r}_N$ are the radii vectors of the point charges modeling a non-spherical tip, and $\mathbf{r}'_1, \dots, \mathbf{r}'_N$ are their mirror images with respect to the plane S' . The parameter k is the screening factor determining an external part of electric field screened by surface charges from penetrating into the polymer film volume. The surface charges for this case include two components $\sigma = \sigma_{\text{pol}} + \sigma_a$: polarization charges (σ_{pol}), and additional charges (σ_a) collected on the surface due to friction. The action of σ_a located on a dielectric surface is simi-

lar to the action of charge distributed on a metal surface with additional parameter k reducing (screening) the basic electric field $\mathbf{E}_0(\mathbf{r})$. We use the following expression for σ_a :

$$\sigma_a = - \sum_{i=1}^n \frac{kQ_i(\mathbf{r} - \mathbf{r}'_i)}{2\pi|\mathbf{r} - \mathbf{r}'_i|^3} \text{ where } \mathbf{r} \in S. \quad (8)$$

Substituting this expression for σ_a together with the expression for σ_{pol} given above in $\sigma = \sigma_{\text{pol}} + \sigma_a$, and inserting Eq. (7) as the basic electric field in Eqs. (1) and (2) for the electric field calculation inside $[\mathbf{E}_{\text{in}}(\mathbf{r})]$ and outside $[\mathbf{E}_{\text{out}}(\mathbf{r})]$ the polymer film, we arrive with the final formula for the traction of the polymer film:

$$\mathbf{T}(\mathbf{r}) = \sigma(\mathbf{r}) \cdot \frac{\mathbf{E}_{\text{in}}(\mathbf{r}) + \mathbf{E}_{\text{out}}(\mathbf{r})}{2}, \text{ where } \mathbf{r} \in S. \quad (9)$$

This formula is used to calculate the pressure (tensile stress) acting on the upper part of the polymer film. Numerical

simulation of the problem indicates that the screening factor value $k \approx 0.9$ produces an electric field inside a polymer film of the order of 10^8 – 10^9 V m⁻¹,¹⁷ well below the electric breakdown threshold.

Equation (9) presents an averaged field instead of $\mathbf{E}_{\text{in}}(\mathbf{r})$ or $\mathbf{E}_{\text{out}}(\mathbf{r})$ excluding self-action.¹³ The expression has two components for tensile (T_{\perp}) and shear (T_{\parallel}) stress. For this case even a weak bias of the AFM tip with respect to the polymer surface (less than 1 V) results in electric fields between 5×10^8 and 5×10^9 V m⁻¹. The distribution of positive charge on the inner lower interface S' must result in electric breakdown through the film leading to the first case. The situation changes qualitatively should the positive charge be concentrated on the upper polymer surface S (presented as surface charges in Fig. 1). This is the case if the tip is weakly biased or if it gains an electric charge frictionally due to its motion above a dielectric surface. A polymer film gains an opposite charge distributed on its surface. These two opposite charges form a capacitor with high intensity field concentrated in a narrow region between the tip, and the polymer film. Again, the height of the film is selected to be $a=30$ nm, but the tip–polymer distances are selected to be $h=0.5$ nm and 0.3 nm. A tip voltage of -1 V results in electric field magnitudes of 2.5×10^9 and 3.3×10^9 V m⁻¹. The results of tensile stress calculation versus x are presented in Figs. 3(c) and 3(d). It is clearly seen that under these conditions the electrostatic pressure overcomes the threshold of plastic deformation in the polymer film. The magnitude of the threshold differs for polymer materials, but for PMMA and PS it is around 25 MPa. This result indicates that the stress occurs even without electric breakdown, and nanostructures are formed by overcoming the plasticity of the material. The width of the nanostructures must follow the distribution of stress (pressure) and should be in the range of 10–50 nm, as can be seen in Fig. 3.

EXPERIMENT

Two different experimental trends for induced nanostructures formation have clearly been observed. The first occurs when an AFM tip is biased at -10 – 50 V with respect to the conductive substrate, so that the potential difference creates an enormously strong electric field of 10^9 – 10^{10} V m⁻¹ resulting in electric breakdown inside a thin polymer film. This is the AFMEN regime^{11,12} accompanied by the electric current through the film in the order of magnitude 100 nA–10 μ A. The stress (pressure) created in the film is described through the set of Eqs. (1)–(3). The AFMEN technique has been verified in polymers with different physical-chemical properties such as: PMMA (980 000 mol wt), PS (2350, 110 000, 2 800 000 mol wt), fluorinated polybenzoxazole, and poly(ethylene terephthalate). A thin layer of the polymer film was spun onto a conductive Au–Pd surface evaporated onto a silicon substrate. The roughness of the films was below 0.2 nm with the average thickness of the film around 30 nm. A conventional Digital Instrument 3100 Dimensions AFM was used to perform nanolithography using highly conductive tungsten carbide AFM tips biased negatively (0–50 V) with respect to the polymer film. A

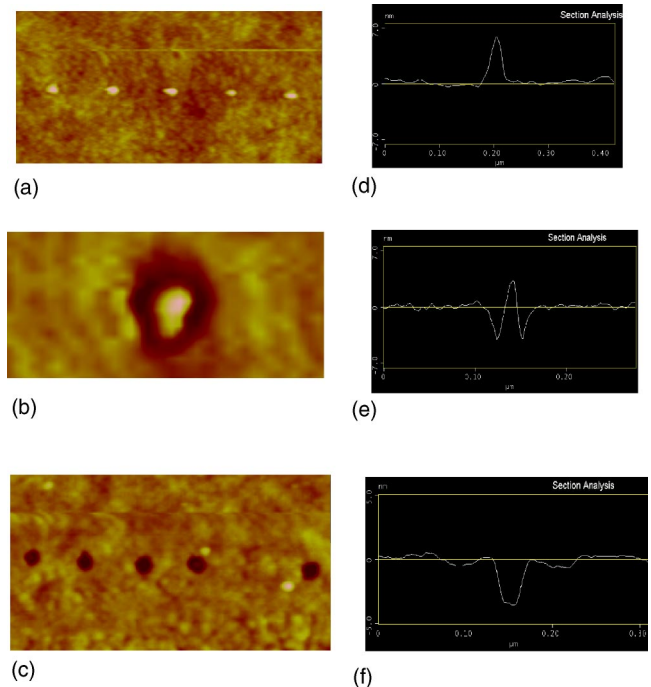


FIG. 4. (Color online) Experimental results of the patterned nanostructures in amplitude-modulated AFMEN. Top view AFM images of (a) dots of 6 nm high and 23 nm wide patterned in polystyrene film (PS, $\epsilon=2.6$, $M_w=110$ k, $T_g=105^\circ$) of 30 nm thickness. Exposure time was 1 s; AFM tip bias was -48 V; average current was 10 nA; (b) dot of 3 nm high inside the hole of 37 nm wide, corresponding to intermediate regime between AFMEN and ablation patterned in polymethylmethacrylate (PMMA, $\epsilon=3.2$, $M_w=960$ k, $T_g=115^\circ$). Exposure time was 1 s for AFM tip bias -26 V with average current 0.1 μ A; (c) set of holes of 4 nm deep, and 37 nm wide patterned in PMMA (ablation mode) using AFM tip bias -30 V, with exposure time 0.5 s, and average current 0.5 μ A. Images (d)–(f) represent the cross section of the images (a)–(c).

Keithley 6485 picoammeter was used to monitor electric current. The height of the nanostructures varies from fractions, to tens of nanometers depending on the magnitude of the electric current through the polymer film. Explanation of the AFMEN process is based on thermal heating, which occurs inside the polymer film described through the solution of the 3D modified heat transfer equation.¹⁶ The heating is the result of electric breakdown through the film accompanied by electric current jumps on several orders of magnitude (from 10 pA to 1–100 nA and greater) followed by surface modification (the formation of lines, grooves, dots, etc.). Four typical regimes are: (1) no patterning, (2) raised nanostructures, (3) intermediate regime: raises inside grooves or raised dots inside holes, and (4) ablation depending on the applied voltage or the electric current. If the current is below 1 nA, normally no surface structures are patterned for bias voltages below 5 V. An increase of applied voltage results in an abrupt increase of the electric current (1–100 nA). This is defined as the AFMEN regime. The solution of the heat transfer equation for a polymer film resting on a conductive substrate suggests that a steady temperature rise above the glass transition temperature can be produced by currents exceeding 5–10 nA for PMMA and PS. The diameter of the

molten polymer region changes nearly linearly with the logarithm of the current.^{11,16} The intermediate regime normally occurs with further current increase for the electric current of the same or greater magnitude than that in the AFMEN regime. An applied voltage above -50 V normally generates breakdown current greater than 100 nA forming distinct depressions and holes in the polymer film. Typical nanostructures created by AFMEN in different polymer films in amplitude-modulated AFM mode are presented in Fig. 4.

The speed of the AFMEN process is determined by two characteristic times: (1) the time required to establish thermal equilibrium in polymer film, τ_h , and (2) the time required polymer melt to flow towards the tip, τ_f . The first one was estimated through the analytical solution of the three-dimensional heat transfer equation inside the polymer film, with Joule current of steady density as a heating source.¹⁶ This time is given by the following expression for $\tau_{\text{heat}} = Ca^2c_p\rho/\kappa$. Here, a is the polymer film thickness, c_p , ρ and κ are the heat capacity, density, and thermal conductivity of the polymer, respectively, and $C \cong 100$. Typical material parameters chosen for the polymer used in our study correspond to the values of τ_h of the order of $0.9 \mu\text{s}$ for PMMA, and $1.4 \mu\text{s}$ for PS. The second characteristic time, τ_f , associated with mass transport of the polymer liquid above its glass transition temperature was estimated using the gradient of the electrostatic pressure. The flow of the (non-Newtonian incompressible) polymer liquid with nonslip boundaries and a power law describing shear thinning, i.e., where viscosity decreases with the rate of shear,¹⁸ was found for PMMA to be $\tau_f = 4.5 \mu\text{s}$ for 10-nm -raised nanostructure for pressure gradient $2.5 \times 10^{13} \text{ Nm}^{-3}$. Based on real-time cantilever deflection signal analysis we conclude that the nanostructures formation occurs is less than $10 \mu\text{s}$. However, the duration of the voltage pulse is $100 \mu\text{s}$, due to the limitations of experimental system. The speed of the polymer raise formation in this experimental trend exceeds all existing single-step nanolithography techniques.

The second experimental trend is distinctly different to AFMEN and polymer ablation. No bias voltage is required to produce nanostructures. Fine lines, $10\text{--}30$ nm wide and $0.2\text{--}1$ nm high, and nanoscopic dots are patterned in 30-nm -polymer film. This process can be implemented only in contact mode AFM when the tip either moves $0.3\text{--}1$ nm or dwells above the surface for a short period of time ranging $0.1\text{--}1$ s. The nanostructures' formation normally occurs as a result of AFM tip motion above the polymer surface with set point magnitude constraining the tip to come closer to the surface depending on the water meniscus size.¹⁹ Another difference between this regime and the AFMEN, is that no depressions are created in this mode. A current of $100 \text{ pA}\text{--}1 \text{ nA}$ was measured through the film, which is substantially smaller than that in AFMEN and is not accompanied by electric breakdown through the film associated with electric current abrupt growth. Nanolines, and nanoscopic dots have been patterned with no applied electric voltage in PMMA and PS polymer films. Typical nanostructures created in this mode are presented in Fig. 5. There is no adequate explanation for this process at the present time. Our tentative hypothesis is associated with electrostatic friction at the nanoscale, and therefore electric charge accumulation by the

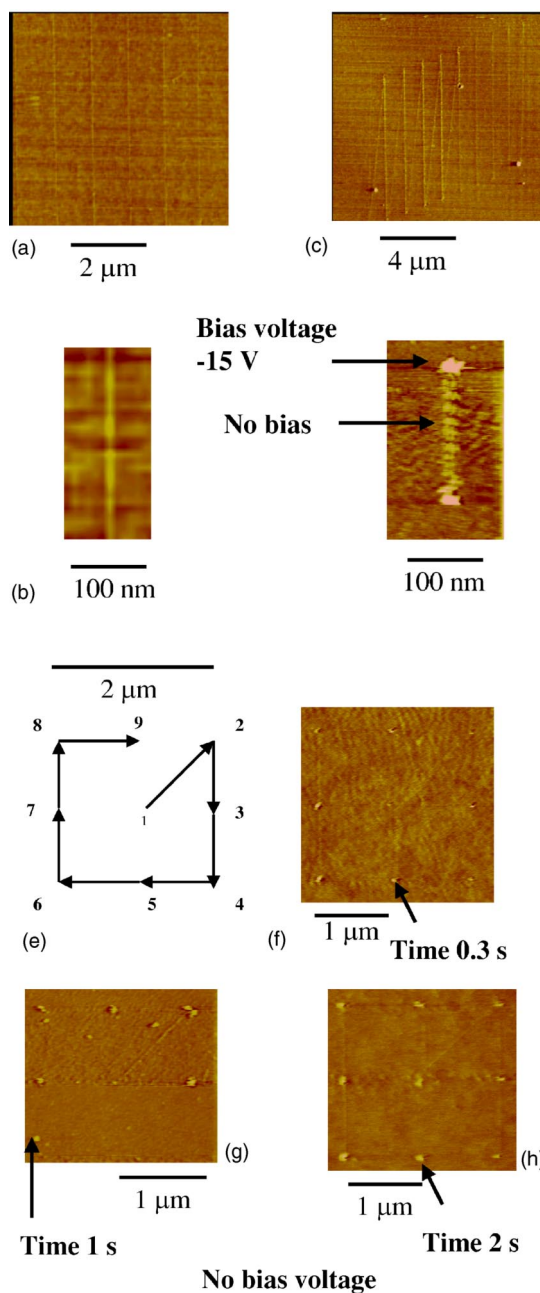


FIG. 5. (Color online) Experimental results of nanostructures patterned in polymer films without external bias: (a) Lines of 25 nm wide and 0.8 nm high patterned in PMMA ($\epsilon=3.2$, $M_w=528\text{k}$, $T_g=115^\circ$); AFM tip velocity was $1 \mu\text{m/s}$ with the average current smaller than 100 pA ; (b) closeup of one of the lines; (c) lines of 47 nm wide and 1 nm high patterned in PS ($\epsilon=2.6$, $M_w=110\text{k}$, $T_g=105^\circ$) without external voltage: the nanolines corresponds to lateral AFM tip motion above the surface; (d) two nanodots patterned in PMMA at the bias voltage -13 V , and 35 nm wide line with voltage turned off. AFM tip velocity was $0.1 \mu\text{ms}^{-1}$; (e) diagram of unbiased tip moving on square of $2 \mu\text{m}$ size above the polymer film: the tip begins moving at point 1, dwelling determined time ($0.3\text{--}2$ s) at each point before stops at point 9; nanoscopic dots patterned in 30-nm -thick PS film by unbiased tip for different dwelling time (f) time was 0.3 s. Dot height varies between 0.5 and 1 nm; (g) time was 1 s. Dot height varies between 0.8 and 1.5 nm; (h) time was 2 s. Dot height varies between 1 and 2.4 nm.

AFM tip during its motion above the polymer film. Triboelectrification, or contact electrification between two metals is well understood and based on electron flow between the metals until their Fermi levels equilibrate.²⁰ The difference of Fermi levels in metals and semiconductors produces a contact potential. Electrons redistribute passing through the contact zone so that one surface gains positive charge while the other gains negative charge. Charge exchange at metal-insulator contacts is not fully understood. The electrons in amorphous dielectric materials are highly localized in the molecules with respect to their distribution in metals and semiconductors. The energy bands in polymer are narrow. A contact redistribution of the charge due to the presence of degenerate or not completely occupied surface states and bulk energy levels is possible between two contacting materials. Macroscopically, this phenomenon is known as electrification by friction. At the nanoscale, a similar contact ionization mechanism may be responsible for spontaneous charge collection by an AFM tip scanning over a polymer film surface in contact mode. The electric charge localized on the surface of PMMA after it has been contacted by a conductive AFM tip has been observed and studied by Terris with co-workers.²¹ Solutions of the Eqs. (1)–(3) indicate that the electric field in the upper part of the polymer film below an AFM tip may exceed 10^9 V m⁻¹, in which, electrostatic traction forces produce rarefaction stress above the plastic deformation threshold. Polymer material in this area, towards the bulk of polymer film, turns plastic. Plastic deformation in polymers below T_g is associated with significant activation energy resulting in a time to produce substantial strain in polymer film which is longer than that for polymer to flow towards the tip in AFMEN process (first trend). This has been experimentally confirmed since the height of nanoscopic dots, formed in PS by an AFM tip without external bias, increases with the increase of dwell time, as demonstrated in Figs. 5(g) and 5(h). It is consistent with earlier observations by Leung and Goh⁹ who reported oriented bundles on the surface of PS, which grew in size, as the tip was allowed to scan for a longer time. The mathematical model describing polymer flow in mixed elastic-plastic mode near glass transition temperature is discussed in Ref. 22. The temperature increase leads to softening of the material lowering the yield stress threshold.

In summary, an exact solution for the electrostatic field inside and outside a planar polymer film has been obtained. The field is a result of the electric field between an AFM tip

and charges accumulated either on the surface of the film through triboelectrification-related processes, or an applied external bias between the tip and interface charges. It has been confirmed experimentally that this solution indeed describes two separate nanolithography mechanisms occurring at the nanoscale in polymer films. In the case when electric breakdown takes place inside the film, polymer features are generated by softened polymer mass transport in a single-step process without external heating either in contact or amplitude-modulated AFM modes. The lateral size of the features patterned in the polymer films varies between 10 and 100 nm with the major factor governing the size being the AFM tip-surface separation. The feature size does not depend substantially on the tip shape or polymer composition used in this type of nanolithography. The process is dependent on the glass transition temperature of the planar polymer film. The second type of nanolithography is related to solid polymer deformation when the AFM tip comes closer to the polymer surface (less than 1 nm) than in standard contact AFM mode. In this case, the electrostatic pressure overcomes the threshold of the material plasticity thus creating the conditions necessary for irreversible changes in the polymer surface. This process is dependent strongly on the AFM tip shape and can be implemented only in contact AFM mode. The size of the features patterned in the film varies between 10–30 nm wide and 0.1–1 nm high. The latter case opens an opportunity for nanostructures' formation in polymer films of arbitrary thickness since the process depends solely on electric charge accumulation on the polymer surface, but not on the breakdown properties as for AFMEN case.

Future work will be dedicated to the specific study of charge accumulation during the process of AFM tip motion in close proximity to polymer surfaces. Patterning nanostructures using triboelectrification at the nanoscale is a concept that may shape the whole area of nanolithography in a broad class of materials.

ACKNOWLEDGMENTS

S.F.L. and P.B.P. acknowledge the support from Air Force Office Sponsored Research Grant No. F49620-02-1-0428, and University of Akron Faculty Research Grant (Fall 2003). R.A.S. acknowledges the support from National Research Council Grant through the COBASE Program. The authors wish to thank R. R. Mallik for the attentive reading of the manuscript and useful comments.

*Electronic address: sfl@physics.uakron.edu

¹Y. Xia, J. A. Rogers, K. E. Paul, and G. M. Whitesides, *Chem. Rev.* (Washington, D.C.) **99**, 1823 (1999).

²S. Y. Chou, L. Zhuang, and L. Guo, *Appl. Phys. Lett.* **75**, 1004 (1999).

³S. Herminghaus, *Phys. Rev. Lett.* **83**, 2359 (1999); *Nat. Mater.* **2**, 11 (2003).

⁴E. Schaffer, T. Thurn-Albrecht, T. Russell, and U. Steiner, *Nature*

(London) **403**, 874 (2000).

⁵M. D. Morariu, N. A. Voicu, E. Schaeffer, Z. Lin, T. P. Russell, and U. Steiner, *Nat. Mater.* **2**, 48 (2003).

⁶Z. Lin, T. Kerle, T. P. Russell, E. Schaeffer, and U. Steiner, *Macromolecules* **35**, 3971 (2002).

⁷H. J. Mamin and D. Rugar, *Appl. Phys. Lett.* **61**, 1003 (1992).

⁸P. Vettiger, M. Despont, U. Drechsler, U. Durig, W. Haberle, M.I. Lutwyche, H.E. Rothuizen, R. Stutz, R. Widmer, and G.K. Bin-

- ning, IBM J. Res. Dev. **44**, 323 (2000).
- ⁹O. M. Leung and M. C. Goh, *Science* **255**, 64 (1992).
- ¹⁰R. Kaneko and E. Hamada, *Wear* **162-164**, 370 (1993).
- ¹¹S. F. Lyuksyutov, R. A. Vaia, P. B. Paramonov, S. Juhl, L. Waterhouse, R.M. Ralich, G. Sigalov, and E. Sancaktar, *Nat. Mater.* **2**, 468 (2003).
- ¹²S. F. Lyuksyutov, P. B. Paramonov, S. Juhl, and R. A. Vaia, *Appl. Phys. Lett.* **83**, 4405 (2003).
- ¹³S. F. Lyuksyutov, R. A. Sharipov, G. Sigalov, and P. B. Paramonov, *cond-mat/0408247*.
- ¹⁴E. K. Dimitriadis, F. Horkay, J. Maresca, B. Kachar, and R. S. Chadwick, *Biophys. J.* **82**, 2798 (2002).
- ¹⁵The stress changes the density (number of polymer molecules per unit volume). Since each molecule has an internal polarizability, the density change must result in a change of total dipole moment, and hence the dielectric permittivity in general. However, in the present model, we assume the permittivity is constant since the polymer liquid is considered to be incompressible.
- ¹⁶The spatial-temporal temperature distribution inside the film requires the solution of 3D heat transfer equation in a cylindrical coordinate system with a Joule heating source. For a more detailed description of the flow of softened non-Newtonian incompressible dielectric liquid with non-slip boundary conditions see Supplementary information Lyuksyutov *et al.*, *Nat. Mater.* **2**, 468 (2003).
- ¹⁷The choice of this specific magnitude of the electric field 10^8 – 10^9 V/m is due to the surface electric charge $\approx 10^{-17}$ C, or 100–150 elementary charges concentrated on the surface. This number was experimentally justified by the authors of Ref. 21 who reported the detection limit of electric force microscopy is 100 electronic charges.
- ¹⁸R. I. Tanner, *Engineering Rheology* (Clarendon, Oxford, 1985).
- ¹⁹S. F. Lyuksyutov, P. B. Paramonov, I. Dolog, and R. M. Ralich, *Nanotechnology* **14**, 716 (2003).
- ²⁰W. R. Harper, *Contact and Frictional Electrification* (Clarendon, Oxford, 1967).
- ²¹B. D. Terris, J. E. Stern, D. Rugar, and H. J. Mamin, *Phys. Rev. Lett.* **63**, 2669 (1989).
- ²²S. F. Lyuksyutov and R. A. Sharipov, *cond-mat/0304190 v 1*.